Improved imaging of electrically conductive solute plumes using a new strategy for physics-based regularization of resistivity imaging problems

Erasmus Oware [1], Stephen Moysey[1], and Taufiquar Khan[2]. [1]Environmental Engineering and Earth Sciences, Clemson University, 340 Brackett Hall, Clemson, SC 29634, USA. [2]Mathematical Sciences, Clemson University.*

Summary:

The ill-posed nature of image reconstruction from sparse and limited data requires that constraints be defined to make the inverse problem tractable. We propose a novel paradigm to physics-based regularization of inverse problems that uses process-based simulations as a soft constraint. We have found that our methodology allows for the reproduction of solute plumes from electrical resistivity surveys with higher fidelity and improved morphology than either standard or coupled inversion, even when the conceptual model underlying our physics-based inversion is incorrect. The new approach therefore appears to be particularly useful when the conceptual model for a process is not yet fully developed, e.g., due to the influence of geologic heterogeneity, or when aspects of the problem are uncertain, such as initial and boundary conditions.

Introduction

Electrical resistivity imaging (ERI) is increasingly employed for monitoring the transport of contaminants and saline tracers (e.g., Slater *et al.*, 2000; Day-Lewis *et al.*, 2003; Singha & Gorelick, 2005) and to evaluate engineered *in situ* remediation (Lane *et al.*, 2004, 2006; Hubbard *et al.*, 2008; Johnson *et al.*, 2010). ERI is an inherently ill-posed inverse problem (Kirsch, 1996), however, with a characteristic non-uniqueness in the mathematical solution. The challenge of ill-posedness and solution non-uniqueness is often addressed by introducing *a priori* constraints in the inverse problem to stabilize the solution (Tikhonov and Arsenin, 1977; Greenhalgh *et al.*, 2006).

A common stabilization approach is to utilize Tikhonov regularization to modify the model space such that solutions with characteristics that are deemed to be appropriate for a particular application are produced. Filters on model space are typically applied to minimize metrics such as a norm of the parameter values or their spatial derivatives to produce images that are, for example, optimally "small", "flat" or "smooth" (e.g., Tikhonov and Arsenin, 1977; Pidlisecky *et al.*, 2007). This traditional regularization strategy introduces artifacts in the solution which may not be consistent with the expected results (Day-Lewis *et. al.*, 2002). For example, smoothness constraints are known to produce images that are overly diffuse (Singha & Gorelick, 2005; Day-Lewis *et al.*, 2007). Furthermore, as illustrated in Figure 1a, traditional regularization constraints are independent of the physical processes and phenomena that generated the particular distribution of parameters that are being imaged.

A contrasting approach to estimation called "coupled inversion" has recently gained interest in the field of geophysical monitoring (Rucker and Ferre, 2004; Kowalski *et al.*, 2005; Ferre *et al.*, 2009; Hinnell *et al.*, 2010). The basic premise of coupled inversion is illustrated in Figure 1b, where a physical process model is coupled to a geophysical instrument model, typically through a rock physics relationship. The observed geophysical data are then used to directly constrain the parameters of the process

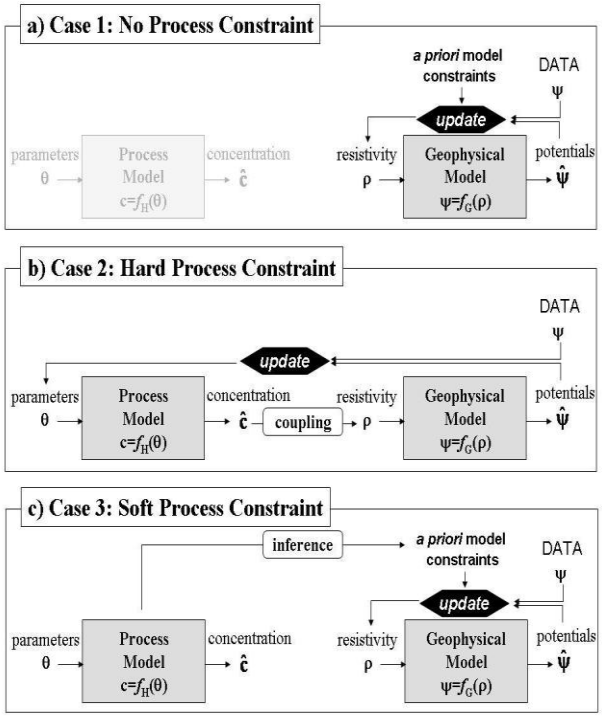

Figure 1: Conceptual illustration of different approaches to utilizing process-based information for imaging solute plumes with ERI: (a) traditional regularization constraints are indpendent of the physical process generating the solute plume; (b) coupled inversion places a hard constraint on the imaging problem as only solute plumes consistent with the process (i.e., transport) model are viable; (c) the proposed soft process constraint extracts information about transport processes generating a solute plume, but can reproduce plumes morphologies that differ from the assumed process model if this is implied by the data.

DOI http://dx.doi.org/10.1190/segam2012-1367.1

model Fowler and Moysey (2011) demonstrated the power of coupled inversion by showing that the parameters of an analytical solute transport model could be estimated from transient apparent resistivity measurements made with a single set of four electrodes, though they also indicated that significant non-uniqueness could occur if the timing and magnitude of the resistivity response are not explicitly considered in the inversion. Similarly, Pidlisecky et al. (2011) used time-lapse tomography surveys to show that improved images of solute plumes could be obtained if parametric models based on solute transport theory are used as a constraint in the inversion.

While coupled inversion allows for the physics of the process being imaged to be integrated into the inverse problem, it applies a hard constraint in the sense that the resulting images must conform to behaviors allowed for by the process simulator. This hard constraint is problematic, particularly when the data suggest that the simulator may be subject to conceptual model errors. The coupled inversion approach is therefore best suited to cases where there is a good understanding of the physical processes being imaged. In this case, the correct structure for the process model can be defined *a priori* and the geophysical data can then constrain the parameters of that model. When the goal of a geophysical survey is to improve our conceptual understanding of processes at a site, coupled inversion is not an appropriate estimation strategy.

There is therefore a subset of geophysical imaging problems that falls between traditional Tikhonov regularization and coupled inversion. In these problems the spatiotemporal distribution of the imaging target is known to obey particular rules of behavior, such as the physics of solute fate and transport, which is not captured by the traditional model filters used in Tikhonov regularization strategies. The details of the processes occurring at a particular site, however, may not be known adequately enough to construct the conceptually accurate model required for coupled inversion. These are *geophysical exploration* problems in the sense that the purpose of the survey is to enhance our conceptual understanding of site-specific processes.

We have formulated an alternate strategy to address these problems whereby the physics of the process generating the target distribution is integrated as a soft process constraint within a standard Tikhonov regularization scheme (Figure 1c). In this abstract we compare the image reconstruction results obtained with this strategy to that obtained with traditional Tikhonov model constraints and coupled inversion. Though the approach is general, we illustrate the method for the specific example where ERI is used to image an electrically conductive solute plume.

Proposed method for ERI with soft process constraints

Our imaging approach is built on a basis-constrained inversion (Vauhkonen *et al*., 1997, Kaipio *et al*., 1999). The key to our method is choosing a set of basis vectors that compactly capture patterns representative of the target-generating process of interest. We take a stochastic approach to this problem whereby we extract the basis from a set of training models. A standard Tikhonov inversion is then conducted in the transformed model space to produce the target image.

Basis-constrained inversion is not a new concept in geophysical imaging (e.g., Milanfar *et al*., 1996). The approach recasts a vector of M model parameters ($\boldsymbol{\sigma}$) as a linear combination of basis vectors, i.e., $\boldsymbol{\sigma} = \mathbf{Bc}$, where each column of the M-by-M matrix $\mathbf{B}$ is a basis vector and $\mathbf{c}$ is a column vector of coefficients that is specific to a particular image. This linear transformation is useful if a basis can be selected that captures the main patterns in $\boldsymbol{\sigma}$ with only a subset of the total columns of $\mathbf{B}$. In this case, the number of non-zero coefficients required to reproduce $\boldsymbol{\sigma}$ at a specified level of accuracy may be much less than M. Thus, proper selection of $\mathbf{B}$ can effectively reduce the number of parameters that need to be estimated for the image reconstruction, which implicitly stabilizes the inversion problem. The challenge is therefore to devise a strategy to choose an appropriate basis $\mathbf{B}$ that is tuned for a specific imaging application.

When imaging a groundwater contaminant or solute, the morphology of the plume is controlled by solute fate and transport processes. Through experience, either with physical or numerical experiments, it is possible to train oneself to recognize physically reasonable morphologies for a solute plume; i.e., we know *a priori* that by definition a "plume" is an object with a compact, elongated shape. By analogy, it is possible to use numerical simulations to create a set of training data from which these patterns can be extracted. These training simulations can be modified to reflect a range of uncertain conceptual models regarding subsurface processes or tuned to account for details captured by site-specific knowledge, such as well log data. By using numerical simulations to produce a set of training data to generate $\mathbf{B}$, we empirically capture information about the spatiotemporal patterns expected for $\boldsymbol{\sigma}$.

Once a basis $\mathbf{B}$ has been defined via the training data, the objective function can be rewritten in terms of the parameter coefficients $\mathbf{c}$ in the projected model space as shown in equation (1).

$$\Phi(\mathrm{c}) = \|\mathbf{d}_{\mathrm{obs}} - f(\mathbf{Bc})\|_2 + \beta\, \mathbf{c}^{\mathrm{T}}\mathbf{W}^{\mathrm{T}}\mathbf{Wc} \qquad (1)$$

Here $\mathbf{d}_{\mathbf{obs}}$ is the measured data, $f(\mathbf{Bc}) = f(\boldsymbol{\sigma})$ is the data predicted using the geophysical model functional $f(-)$ for

DOI http://dx.doi.org/10.1190/segam2012-1367.1

the specific parameters $\boldsymbol{\sigma}$, β is the regularization parameter, and **W** is a regularization operator. We expect the solution to be sparse in the transformed space, so use an operator that selects for small values of the parameters in **c**, i.e., a diagonal matrix **Σ**. We also expect, however, that a solute plume will not have erratic, discontinuous behaviors through the subsurface, so penalize for roughness by also minimizing the second spatial derivative of $\boldsymbol{\sigma}$ by applying a smoothness operator $\mathbf{G}^*$, i.e., $\mathbf{G\sigma} = \mathbf{GBc} = \mathbf{G}^*\mathbf{c}$. A second regularization parameter γ must also be added in equation (2) to balance the two model constraints.

$$\mathbf{W} = \boldsymbol{\Sigma} + \gamma\, \mathbf{G}^*\mathbf{B} \qquad (2)$$

The objective function given in equation (1) can be minimized using standard optimization techniques to estimate the coefficients **c** under the basis constraint. Afterward, the final reconstructed image can be obtained from the product of **B** and the estimated coefficients.

Numerical comparison of imaging algorithms

We compare the inversion results obtained from our proposed basis-constrained approach to those obtained using standard Tikhonov regularization and coupled inversion for the problem where a solute plume is imaged using ERI. For these numerical examples, we used the program SGSIM (Deutsch & Journel, 1998) to generate a 50 m by 50 m two-dimensional random field of hydraulic conductivity values using an isotropic exponential variogram model with correlation lengths of 25m. Flow velocities were calculated through this medium by applying a uniform hydraulic gradient on two opposing boundaries and assuming no flow conditions on the remaining two boundaries. Two advection dominated transport cases were considered. In the first case, a transport simulation was performed with a single source zone located at x=5m and y=20m to generate the true plume shown in the first column of Figure 2a. In contrast, two solute source zones (x=5m, y=15m and x=8m, y=25m) were used to generate the strongly bimodal plume shown in the first column of Figure 2c. The following version of Archie's law (Archie, 1942) was used to transform the concentrations to electrical conductivities:

$$\sigma(x,y,t) = 1.5x10^{-4}n^{1.3}c(x,y,t) \qquad (3)$$

where n is the porosity, assumed to be 0.3. Electrical resistivity data were generated for each of these "true" models using the forward model of Pidlisecky *et al*. (2007), which had been modified for two-dimensional problems. The data consisted of measurements collected from 16 equally spaced electrodes located along the top (i.e., ground) surface of the electrical conductivity model.

Resistivity imaging of the solute plumes using the traditional Tikhonov regularization was completed using a version of the code from Pidlisecky *et al*. (2007) that was modified to two-dimensions. A model smallness constraint was used to force $\boldsymbol{\sigma}$ toward the background conductivity value in the aquifer and a model smoothness constraint was used in generating these inversions. The ERI results obtained for both synthetic plume 1 and 2 are shown in column 2 of Figure 2. In both cases, it is clear that the plumes are overly smooth compared to the true case. After using equation (3) to back transform electrical conductivity to concentration, it is also clear that the concentrations estimated from ERI significantly underestimate the true plume concentrations (Figure 3). This particular behavior is likely a result of the combination of model constraints used in this problem, but poor estimation of solute concentrations from ERI is a well-documented phenomenon (e.g., Singha and Gorelick, 2005).

For the coupled inversion problem, we used an analytical transport model for one-dimensional flow given by De Josselin De Jong (1958), where the dispersivities are fixed based on the EPA TACO regulation:

$$c(x,y,t) = \frac{m}{0.231\pi v_x{}^2 t^2}\exp\left\{-\frac{[(x-x_0)-v_x t]^2}{0.4 v_x{}^2 t^2} - \frac{(y-y_0)^2}{0.133 v_x{}^2 t^2}\right\}, \qquad (4)$$

where, tracer mass m is slug injected at a point (x_0,y_0) with a velocity v_x. The concentration at any location (x,y) after time t of tracer injection is c(x,y,t). We again used equation (3) to convert between concentration and electrical conductivity. In this case, we assumed that the source location of the plume (x_o,y_o) was known *a priori*, so

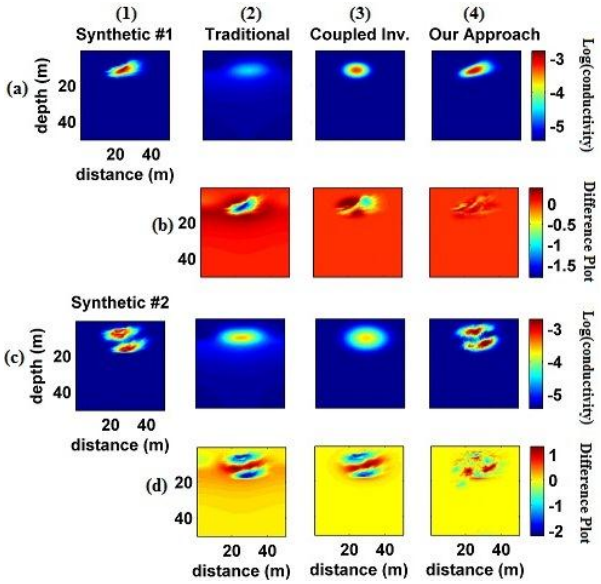

Figure 2: Comparison of a true plume (1) to images obtained via three different inversion strategies: traditional Tikhonov smoothness constraint (2), coupled inversion (3), and our physics-based basis-constrained inversion (4). Tomograms in row (a) are for synthetic plume #1 and those in row (c) represent synthetic plume #2. Rows (b) and (d) are their respective difference plots.

DOI http://dx.doi.org/10.1190/segam2012-1367.1

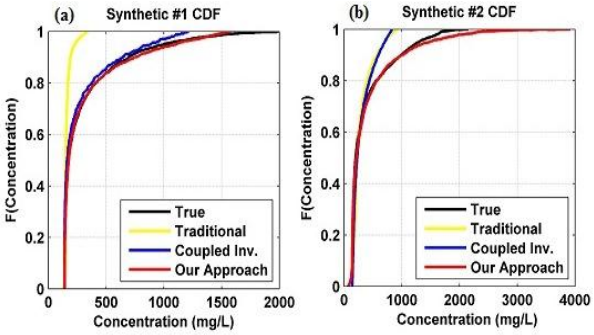

Figure 3: Comparison of the commulative distribution curves of estimated concentration for the three different inversion strategies: (a) synthetic plume #1 and (b) synthetic plume #2.

there are only three parameters that control the plume: the mass (m), flow velocity (v_x), and length of time between when the plume was released and when it is imaged (t). The problem is overdetermined in this case, so the solution can be found by minimizing an objective function with only a data misfit term. This problem was solved using the trust-region-reflective optimization algorithm (lsqnonlin) in MATLAB (Coleman & Li, 1996).

The results of the coupled inversion are shown in the third column of Figure 2. The hard constraint of the transport model allows the coupled inversion to obtain a reasonable estimate of the first synthetic solute plume. It is also clear from Figure 3 and the RMSE values reported in Table 1 that the concentration estimates are much improved compared to the standard Tikhonov regularization result. The same is not true, however, for the second synthetic plume. In this case, the conceptual model used in the coupled inversion is incorrect – the transport model assumes that the plume is unimodal, whereas it is actually bimodal. As a result, the coupled inversion causes the estimated plume to be much larger than either of the two small plumes in the true case. This redistribution of mass over a large region causes the concentrations to be significantly underestimated. In fact, the coupled inversion has roughly the same poor performance observed for the standard Tikhonov inversion. This example illustrates the fact that coupled inversion has limited value when the conceptual model underlying the imaged phenomenon is incorrect.

The training data used to create the basis vectors for our proposed inversion methodology were generated in a similar procedure as that used for the true plumes. There were, however, several key differences. In particular, the correlation lengths of the hydraulic conductivity field were not assumed to be known *a priori*. Instead, we generated 4 sets of 100 random fields for correlation lengths of 10, 15, 20 and 30 m. We also assumed that we knew the hydraulic gradient and the single solute source location for the plume generated in synthetic plume 1, but did not include a second source zone for generating the basis for the second synthetic solute plume. In this way, our conceptual model used to generate the basis for the second synthetic test was intentionally incorrect. The starting coefficients in the inversion are given by transforming the initial conductivity estimate ($\boldsymbol{\sigma}_o$), i.e., $\mathbf{c}_0 = \boldsymbol{\sigma}_0\mathbf{B}$, which we choose here to be a homogenous value equal to the *in situ* background conductivity of the aquifer. The basis-constrained inversion was performed using the trust-region-reflective optimization algorithm (lsqnonlin) in MATLAB.

The inversions obtained using the basis constrained approach are clearly superior to those obtained with either of the other two estimation methodologies (Figure 2 and Table 1). Both the overall morphology of the plume and concentration values are estimated accurately for the first synthetic plume. Impressively, the proposed method is also able to capture the bimodal morphology of the second synthetic plume despite the fact that the conceptual model used to generate the training data for the basis functions was incorrect. The estimated concentration values are slightly overestimated in this case, but the overall match is excellent except at the highest concentration levels (Figure 3).

Table 1: Root mean square error (RMSE) of concentration for each ERI inversion example.

Synthetic Plume Case	ERI Estimation Method		
	Traditional	*Coupled*	*Basis Constraint*
#1	0.212	0.140	0.043
#2	0.346	0.273	0.165

Conclusions

We proposed a novel paradigm for the physics-based regularization of inverse problems. Our approach uses non-parametric basis functions in constraining the inversion procedure that are derived from numerical simulations of the process generating the target to be imaged. Our numerical illustration clearly demonstrates the efficacy of our new basis constraint approach to imaging problems. In comparing the plume morphology and estimated solute concentrations, the new basis-constrained methodology consistently outperformed the other methods. This was particularly impressive in the instance of synthetic plume #2, where the conceptual model used to generate the basis vectors was inaccurate but our approach was still able to capture the bi-modality of the plume. There are many questions that must still be answered regarding the generality and robustness of this new approach to physics-based regularization of inverse problems. Regardless, we believe that the strategy will provide new directions for developing regularization strategies for dynamic systems that crosses disciplinary boundaries in inverse theory.

DOI http://dx.doi.org/10.1190/segam2012-1367.1

http://dx.doi.org/10.1190/segam2012-1367.1

EDITED REFERENCES

Note: This reference list is a copy-edited version of the reference list submitted by the author. Reference lists for the 2012 SEG Technical Program Expanded Abstracts have been copy edited so that references provided with the online metadata for each paper will achieve a high degree of linking to cited sources that appear on the Web.

REFERENCES

Archie, G. E., 1942, The electrical resistivity log as an aid in determining some reservoir characteristics: Transactions of the American Institute of Mining, Metallurgical and Petroleum Engineers, **146**, 54–62.

Binley, A., G. Cassiani, R. Middleton, and P. Winship, 2002, Vadose zone flow model parameterisation using cross-borehole radar and resistivity imaging: Journal of Hydrology (Amsterdam), **267**, 147–159.

Coleman, T. F., and Y. Li, 1996, An interior, trust region approach for nonlinear minimization subject to bounds: SIAM Journal on Optimization, **6**, 418–445.

Day-Lewis, F. D., Y. Chen, and K. Singha, 2007, Moment inference from tomograms: Geophysical Research Letters, **34**, L22404, doi:10.1029/2007GL031621.

Day-Lewis, F. D., J. M. Harris, and S. M. Gorelick, 2002, Time-lapse inversion of crosswell radar data: Geophysics, **67**, 1740–1752.

Day-Lewis, F. D., J. W. Lane, Jr, J. M. Harris, and S. M. Gorelick, 2003, Time-lapse imaging of saline-tracer transport in fractured rock using difference-attenuation tomography: Water Resources Research, **1290**, doi:10.1029/2002WR0011722.

de Josselin de Jong, G., 1958, Longitudinal and transverse diffusion in granular deposits: EOS, Transactions American Geophysical Union, **39**, 67–74.

Deutsch, C. V., and A. G. Journel, 1998, Geostatistical software library and user's guide: Oxford University Press.

Ferré, T., L. Bentley, A. Binley, N. Linde, A. Kemna, K. Singha, K. Holliger, J. A. Huisman, and B. Minsley, 2009, Critical steps for the continuing advancement of hydrogeophysics: EOS, Transactions American Geophysical Union, **90**, no. 23, 200, doi:10.1029/2009EO230004.

Fowler, D. E., and S. M. J. Moysey, 2011, Estimation of aquifer transport parameters from resistivity monitoring data within a coupled inversion framework: Journal of Hydrology (Amsterdam), **409**, 545–554.

Greenhalgh, S. A., Z. Bing, and A. Green, 2006, Solutions, algorithms and inter-relations for local minimization search geophysical inversion: Journal of Geophysics and Engineering, **3**, 101–113.

Hinnell, A. C., T. P. A. Ferré, J. A. Vrugt, J. A. Huisman, S. Moysey, J. Rings, and M. B. Kowalsky, 2010, Improved extraction of hydrologic information from geophysical data through coupled hydrogeophysical inversion: Water Resources Research, **46**, W00D40, doi:10.1029/2008WR007060.

Hubbard, S. S., K. Williams, M. Conrad, B. Faybishenko, J. Peterson, J. Chen, P. Long, and T. Hazen, 2008, Geophysical monitoring of hydrological and biogeochemical transformations associated with Cr(VI) biostimulation: Environmental Science & Technology, **42**, 3757–3765, doi:10.1021/es071702s.

Johnson, T. C., R. J. Versteeg, A. Ward, F. D. Day-Lewis, and A. Revil, 2010, Improved hydrogeophysical characterization and monitoring through parallel modeling and inversion of time-domain resistivity and induced polarization data: Geophysics, **75**, no. 4, 27–41, doi:10.1190/1.3475513.

Kaipio, J. P., V. Kolehmainen, M. Vauhkonen, and E. Somersalo, 1999, Inverse problems with structural priori information: Inverse Problems, **15**, 713–729.

Kirsch, A., 1996, An introduction to the mathematical theory of inverse problems: Springer.

Lane, J. W., Jr., F. D. Day-Lewis, and C. C. Casey, 2006, Geophysical monitoring of field-scale vegetable oil injections for biostimulation: Ground Water, **44**, 430–443, doi:10.1111/j.1745-6584.2005.00134.x.

Lane, J. W., Jr., F. D. Day-Lewis, R. J. Versteeg, and C. C. Casey, 2004, Object based inversion of crosswell radar tomography data to monitor vegetable oil injection experiments: Journal of Environmental & Engineering Geophysics, **9**, 63–77.

Kowalsky, M. B., S. Finsterle, J. Peterson, S. Hubbard, Y. Rubin, E. Majer, A. Ward, and G. Gee, 2005, Estimation of field-scale soil hydraulic and dielectric parameters through joint inversion of GPR and hydrological data: Water Resources Research, **41**, W11425, doi:10.1029/2005WR004237.

Milanfar, P., W. C. Karl, and A. S. Willsky, 1996, A moment-based variational approach to tomographic reconstruction: IEEE Transactions on Image Processing, **5**, 459–470.

Pidlisecky, A., E. Haber, and R. Knight, 2007, A 3D resistivity inversion package: Geophysics, **72**, no. 2, H1–H10.

Pidlisecky, A., S. Kamini, and F. D. Day-Lewis, 2011, A distribution-based parametrization for improved tomographic imaging of solute plumes: Geophysical Journal International, **187**, 214–224.

Rucker, D. F., and T. P. A. Ferré, 2004, Parameter estimation for soil hydraulic properties using zero-offset borehole radar: Analytical method: Soil Science Society of America Journal, **68**, 1560–1567.

Singha, K., and S. M. Gorelick, 2005, Saline tracer visualized with electrical resistivity tomography: Field scale moment analysis: Water Resources Research, **41**, W05023, doi:10.1029/2004WR003460.

Slater, L., A. M. Binley, W. Daily, and R. Johnson, 2000, Cross-hole electrical imaging of a controlled saline tracer injection: Journal of Applied Geophysics, **44**, 85–102.

Tikhonov, A. N., and V. Y. Arsenin, 1977, Solutions of ill-posed problems: John Wiley & Sons.

Vauhkonen, M., J. P. Kaipio, E. Somersalo, and P. A. Karjalainen, 1997, Electrical impedance tomography with basis constraints: Inverse Problems, **13**, 523–530.